NASA TECHNICAL NOTE

NASA TN D-3361

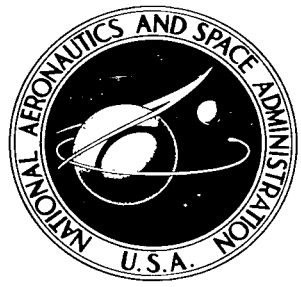

NASA TN D-3361

RADIOFREQUENCY POWER TRANSFER TO ION-CYCLOTRON WAVES IN A COLLISION-FREE MAGNETOPLASMA

by Donald R. Sigman

Lewis Research Center

Cleveland, Ohio

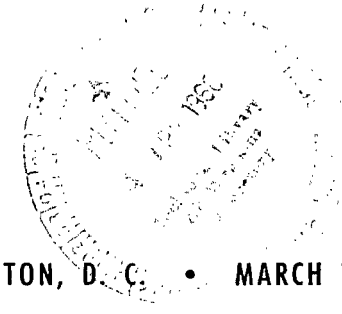

NATIONAL AERONAUTICS AND SPACE ADMINISTRATION • WASHINGTON, D. C. • MARCH 1966

NASA TN D-3361

RADIOFREQUENCY POWER TRANSFER TO ION-CYCLOTRON WAVES IN A COLLISION-FREE MAGNETOPLASMA

By Donald R. Sigman

Lewis Research Center
Cleveland, Ohio

NATIONAL AERONAUTICS AND SPACE ADMINISTRATION

For sale by the Clearinghouse for Federal Scientific and Technical Information
Springfield, Virginia 22151 – Price $0.35

RADIOFREQUENCY POWER TRANSFER TO ION-CYCLOTRON WAVES IN A COLLISION-FREE MAGNETOPLASMA

by Donald R. Sigman

Lewis Research Center

SUMMARY

With the Fourier integral theory developed by T. H. Stix, calculations were made on power transfer from a radiofrequency coil to an ion-cyclotron wave in a cold collisionless cylindrical plasma. The effects of varying parameters such as static magnetic field, electron density, radiofrequency, plasma and coil radius, and wavelength are discussed. It is shown that there is an optimum radiofrequency coil wavelength for maximum power transfer, and curves are presented to facilitate the selection of this wavelength. The importance of placing the radiofrequency coil as close to the plasma as possible is also shown. Finally, a comparison is made between calculations from the above mentioned Fourier integral theory and a former Fourier-Bessel series theory (also developed by Stix). The two theories are not found to be in agreement.

INTRODUCTION

The generation of ion-cyclotron waves in a plasma column is of interest to experimentalists concerned with the heating of plasma through collisionless processes. This report contains calculations from a theoretical plasma model of the effect of various plasma parameters on the power transferred from a radiofrequency coil to the ion-cyclotron wave in the plasma. In this model, the radiofrequency coil is of finite length, and it is wrapped around an infinitely long plasma column surrounded by a vacuum and immersed in a steady uniform magnetic field parallel to the axis of the column. The assumption that the plasma is of constant density, cold, and collision free is made in the model.

In the region underneath the coil, power is transferred from the radiofrequency coil to the ion-cyclotron wave. This wave then propagates unattenuated out both ends of the coil and down the plasma column. Since the plasma model is cold, all energy from the coil shows up as electromagnetic energy of the wave.

By using the previous physical model and assuming, in addition, that the electron has zero mass, T. H. Stix (ref. 1) derived expressions for the power transferred to ion-cyclotron waves.

Stix, by using a Fourier integral, represented the current sheet distribution in the finite length coil by an infinite series of current sheets, each infinitely long. The wavelengths of these current sheets ranged from zero to infinity, and the relative strength of each current sheet was determined by the Fourier integral. Since the electric fields associated with each of these infinitely long current sheets can be easily calculated, it was then possible to get an expression for the field of the finite length coil by superposing the fields of all the infinitely long current sheets. This technique resulted in an integral for the electric field of the finite length coil. This integral was solved by using contour integration to arrive at the final expressions for both the real and imaginary parts of the field (i.e., those parts of the field in phase with and 90° out of phase with the current in the current sheet). The power transferred to the wave was then computed by averaging over the length of the coil the product of the current in the finite current sheet and the real part of the electric field at the current sheet.

Stix formerly used another technique that employed a Fourier series to calculate power transfer to the ion-cyclotron wave (ref. 2). A comparison of the results of this former technique with those of the Fourier integral technique is given in the appendix.

In this report, the results of digital computer calculations from the expressions derived in reference 1 are presented. The effects of the following plasma parameters on power transfer were studied: plasma wavelength, plasma mode, radiofrequency coil radius and length, and magnetic field. An attempt has been made to present the results of the calculations in such a way that they are an aid to an experimentalist both in designing an efficient means for power transfer from a radiofrequency coil to the plasma wave and in interpreting the data.

SYMBOLS

The cgs-gaussian units are used throughout.

a	length of one-half of radiofrequency exciting coil
B	magnetic field strength
B_0	magnetic field at ion-cyclotron particle resonance
c	velocity of light
E_θ°	see eq. (4b)
E_θ^V	θ component of vacuum electric field, see eq. (4a)
e	electronic charge
F	radiofrequency coil radius correction factor
G	defined by eq. (12b)

I_1 modified Bessel function of first kind

J_1 Bessel function of first kind

j_ℓ magnitude of radiofrequency coil current

j^* radiofrequency coil current per unit length

K_1 modified Bessel function of second kind

k axial wave propagation constant (wave no.) in plasma

k_n see eqs. (8) and (9)

$k_{0\ell}$ axial radiofrequency coil current propagation constant (wave no.)

m_I mass of hydrogen ion

n_e electron density

P_ℓ total power transferred to ion-cyclotron waves from radiofrequency coil

P^* relative power transfer ($2\pi a^2 j_\ell^2 P^* = P_\ell$)

p plasma radius

R relative power transfer factor, see eq. (6d)

r radial cylindrical coordinate

$S_i(\eta)$ shape factor for imaginary power transfer, see eq. (6a)

$S_r(\eta)$ shape factor for real power transfer, see eq. (6b)

s radiofrequency coil radius

t time

z axial cylindrical coordinate

η $2a(k_{0\ell} - k_n)$

θ azimuthal cylindrical coordinate

ν radial wave number

Π_I ion plasma frequency

ω radiofrequency/2π

Ω ω/Ω_I

Ω_I eB/m_Ic

THEORY

The axis of the plasma cylinder is designated the z-axis and cylindrical coordinates are used. The steady magnetic field is directed along this z-axis. The exciting radiofrequency coil for the system has a length 2a, surrounds the plasma cylinder, and is centered at $z = 0$ (see fig. 1). The aximuthal current per unit length in the coil is to be represented by the following Fourier series:

$$j^* = \sum_{l=1}^{\infty} j_l e^{i(k_{0l}z-\omega t)} \qquad -a \leq z \leq a \tag{1a}$$

$$j^* = 0 \qquad |z| > a \tag{1b}$$

In order to represent a finite length coil in a single equation, Stix further decomposed each Fourier current component in equation (1) into its Fourier integral spectrum so that

$$j^* = \sum_{l=1}^{m} j_l e^{i(k_{0l}-\omega t)} = \sum_{l=1}^{m} j_l \int_{-\infty}^{\infty} \frac{\sin(k - k_{0l})a}{\pi(k - k_{0l})} e^{i(kz-\omega t)}\, dk \tag{2}$$

This led to the following expression for the electric field E_θ at the radius of the coil:

$$(E_\theta)_{r=s} = \sum_{l=1}^{m} \frac{1}{\pi} j_l \int_{-\infty}^{\infty} \left(E_\theta^v\right)_{r=s} \frac{\sin(k - k_{0l})a}{(k - k_{0l})} e^{i(kz-\omega t)} dk \tag{3}$$

where

$$E_{\theta\ r=s}^{v} = \frac{4\pi i\omega}{c^2} j^* s I_1(ks) K_1(ks) + E_\theta^o \tag{4a}$$

$$\left(E_\theta^o\right) \equiv \frac{4\pi i\omega}{c^2} j^* s K_1^2(ks) \frac{\nu J_1'(\nu p) I_1(kp) - k I_1'(kp) J_1(\nu p)}{k J_1(\nu p) K_1'(kp) - \nu J_1'(\nu p) K_1(kp)} \tag{4b}$$

The $\left(E_\theta^v\right)_{r=s}$ is the θ component of the vacuum electric field at $r = s$ when the coil is assumed to be infinitely long and to have a current distribution

per unit length $j_\ell e^{i(kz-\omega t)}$. By working from equation (3), Stix was able to derive the following expression for the power transferred to the n^{th} natural mode of the plasma wave when all the j_ℓ's have been assumed zero except one:

$$P_\ell = -i(2\pi sa^2)j_\ell\left[(k - k_n)E^v_{\theta r=s}\right]_{k=k_n}\left[S_r(\eta) - iS_i(\eta)\right]$$

$$= +(2\pi a^2)j_\ell^2 R\left[S_r(\eta) - iS_i(\eta)\right] \tag{5}$$

$$S_r(\eta) \equiv \frac{2(1 - \cos\eta)}{\eta^2} \tag{6a}$$

$$S_i(\eta) \equiv \frac{2(\eta - \sin\eta)}{\eta^2} \tag{6b}$$

$$\eta \equiv 2(k_{0\ell} - k_n)a \tag{6c}$$

$$R \equiv -i(k - k_n)\left(E^v_{\theta r=s}\right)_{k=k_n}\frac{s}{j_\ell} \tag{6d}$$

The real part of P_ℓ corresponds to resistive plasma loading, which is the power transferred to the plasma wave as measured in the laboratory. Thus,

$$\text{Re } P_\ell = 2\pi a^2 j_\ell^2 R S_r(\eta) \tag{7}$$

The natural modes are determined by finding the conditions under which E_θ in the plasma under the infinitely long coil remains nonzero when $j^* = 0$. This condition is met when the denominator of equation (4b) is zero:

$$kJ_1(\nu p)K_1'(kp) - \nu J_1'(\nu p)K_1(kp) = 0 \tag{8}$$

The dispersion relation for ion-cyclotron waves in the plasma is given by equations (5) to (9) in reference 1:

$$\frac{\nu^2c^2}{\Pi_I^2} = \frac{\dfrac{\omega^4}{\Omega_I^4} - \dfrac{\omega^2}{\Omega_I^2}\left(2\dfrac{k^2c^2}{\Pi_I^4} + \dfrac{k^4c^4}{\Pi_I^4}\right) + \dfrac{k^4c^4}{\Pi_I^4}}{\dfrac{\omega^2}{\Omega_I^2}\left(1 + \dfrac{k^2c^2}{\Pi_I^2}\right) - \dfrac{k^2c^2}{\Pi_I^2}} \tag{9}$$

The simultaneous solution of equations (8) and (9) gives the values ν_n and k_n for the n^{th} natural mode of the plasma. These values were then used in equation (6d) to compute R on the 7094 digital computer. At $k = k_n$, both numerator and denominator of equation (6d) are zero. This indeterminancy is eliminated in the calculations through use of l'Hospital's rule with respect to k.

DISCUSSION OF RESULTS

For the purpose of the discussion that follows, it should be noted that the equation for power transfer (eq. (7)) contains three terms of interest: $2\pi a^2 j_l$, R, and $S_r(\eta)$. The function $S_r(\eta)$, which is called the "shape factor" by Stix, is the only term which contains k_{0l}, and it is a maximum when $k_{0l} = k_n$ (see fig. 2). The term R is a function of k_n, s, p, n_e, and Ω, but not k_{0l}. Thus, the maximum $RS_r(\eta)$ product is achieved by selecting k_{0l} equal to the value of k_n for which R is a maximum, since under this condition both R and $S_r(\eta)$ are maximum.

In the following sections, the effects of static magnetic field, wavelength and radii of the plasma and radiofrequency coil, and plasma density on radiofrequency power transfer are discussed. Also, plasma modes other than the primary mode are compared to the primary mode, and calculations are made with nonsinusoidal radiofrequency coil current distributions as well as with sinusoidal distributions. In equation (1), it is stated that the current sheet is a traveling wave current sheet in the +z direction. The results presented in the following sections are the same if the current sheet is assumed to travel in the -z direction. Thus, if one wishes results for a standing wave current sheet, he may to a good approximation simply add the contributions from the positive and the negative z-directed waves. In doing this, the cross terms, which are very small, are neglected.

Different Plasma Modes

The simultaneous solution of equations (8) and (9) gives an infinite number of values for ν_n, and for each value of ν_n there is a contribution to power absorption. However, it was found numerically that only the contribution for the mode with the lowest value of ν_n was of significance. In all cases studied, the contribution of the lowest mode was more than ten times that of the next highest mode; the shapes of the curves presented are not affected by inclusion of the higher modes. Thus, all curves shown in this report are from lowest order mode calculations (i.e., n = 1).

Magnetic Field

The dependence of R on the magnetic field for a typical laboratory plasma is shown in figure 3. Relative power absorption ($P^* = RS_r(\eta)$) against Ω is given in figure 4. In this situation, $j_1 = 1$ (all other $j_l = 0$), $k_{01} = 0.140$ per centimeter, $a = 2\pi/k_{01}$, $n_e = 5\times10^{11}$ per cubic centimeter, plasma radius = 2.5 centimeters, coil radius = 7.5 centimeters, and $\omega = 2\pi\times6.5\times10^6$ per second ($B_0 = 4200$ G). The relative power absorption curve in figure 4 is very much like a plot of $S_r(\eta)$ against Ω (also presented in fig. 4). However, the relative power absorption curve has a narrower half-width, and the magnetic field at maximum power absorption is less than the magnetic field at the peak in the $S_r(\eta)$ against Ω plot (i.e., where $\eta = 0$).

Even though the calculations for figures 3 and 4 have been made by using

specific values of the parameters ω, s, p, k_{01}, and n_e, the basic shape of these curves is preserved for other values of the parameters. Different values of ω, s, or p affect the magnitude of R for a given Ω; n_e largely determines the value of Ω where R is a maximum (Ω decreases as n_e increases). Different values of k_{01} move the peak of $S_r(\eta)$ with respect to Ω.

In the derivation for R (eq. (5d)), the displacement current term from Maxwell's equations was neglected. For large magnetic fields (when the phase velocity ω/k is no longer negligibly small compared to the velocity of light), displacement current may be included by replacing k in the expression for R by $k^2 - [(\omega^2/c^2)]^{1/2}$. For $B_0 = 75$ kilogauss ($\omega = 2\pi \times 1.16 \times 10^8$ sec^{-1}) and k = 0.15 per centimeter, $(\omega/k)^2 = 0.24 \times 10^{20} = 0.26\ c^2$; therefore, the curve P^* against Ω is not changed from that of figure 4 where $B_0 = 4.2$ kilogauss.

Plasma Wavelength and Radiofrequency Coil Length

In studying the effects of coil length on plasma power absorption, two cases are considered. For case A, the physical length 2a of the coil is held constant, and the value of k_{01} in the principal Fourier component of the current distribution as given by equation (1a) is varied. In case B, the physical length of the coil is varied but phased for two wavelengths so that $a = 2\pi/k_{01}$.

Figures 5(a) to (d) show R against k_n for case A for a range of the variables p and n_e with s held constant. From these curves, it is seen that there is a value of k_n which makes R a maximum. This point of maximum R, however, occurs at different values of k_n for different values of p, n_e, and s. For larger values of s, the peak was found to occur at smaller values of k_n such that when n_e is held constant the product $k_n s$ at the peak is a constant. The position of the peak is less sensitive to changes in p. For high densities ($n_e > 10^{12}$ cm^{-3}), the peak occurs at larger values of k_n, but it does not vary significantly with density for $n_e < 10^{12}$ per cubic centimeter.

For case B, $P_1 = 2\pi a^2 j_1^2 R S_r(\eta)$ and $a = 2\pi/k_{01}$. When $k_{01} = k_n$ (i.e., when $S_r(\eta)$ is a maximum), then $P_1 \sim a^2 R = 4\pi^2/k_n^2\ R$. Figures 6(a) to (d) show R/k_n^2 as a function of k_n for a range of the variables p and n_e with s again set equal to 10 centimeters. Again there are maxima in the curves, which indicate a point of maximum power transfer. The dividing of R by k_n^2 moves the peak to lower k_n values (compare figs. 6(a) and (b)). Qualitatively, the effects of s, p, and n_e on the maximum power points are the same for case B as for case A.

Since figures 5 and 6 are for a fixed value of s = 10 centimeters, a correction factor is needed if the curves are to be useful for other values of s. We therefore define a function $F(k_n s) = [k_n s K_1(k_n s)]^2$, which contains the entire dependence of power on s. This function is plotted in figure 7 for a range of s values. Corrections to the values in figures 5 and 6 for values of $s \neq 10$ may be made by multiplying by the correction factor $F(k_n s)/F(10k_n)$.

All the curves in figures 5 and 6 are plotted with k_n as the abscissa. This is a useful form for designing an experiment. For interpreting data,

however, a more useful variable is Ω, which is defined by

$$\frac{1}{\Omega^2} = 1 + \frac{\pi_I^2}{k_n^2 c^2} \tag{10}$$

Equation (10) permits the evaluation of k_n in terms of measurable quantities π_I and Ω.

Plasma Density

Figure 8 shows the effects of varying the density on power adsorption. For curve (a), the value of k_{01} was set at a fixed value (0.140 cm^{-1}) and "peak" relative power transfer (P^* at $k_n = k_0$) was plotted. For curve (b), the value of k_{01} was adjusted for each density so that k_{01} was equal to the value of k_n which gave a maximum in the R against k_n curve (fig. 5(a)). For curve (c), the value of k_{01} was adjusted to the value of k_n which gave a maximum in the R/k_n^2 against k_n curve (fig. 6(a)).

The conclusion is that over the density range 3×10^9 per cubic centimeter $< n_e < 5\times10^{12}$ per cubic centimeter power absorption is a weak function of density, but it drops off rapidly if an attempt is made to go to higher densities.

Figure 9 shows the values of Ω for "peak" relative power absorption against density when $k_{01} = 0.140$ per centimeter.

Plasma and Radiofrequency Coil Radius

Figure 10 shows the effect of plasma and coil radius on "peak" relative power absorption by the plasma. It is seen that when the radiofrequency coil radius s is held constant, power absorption rises faster than $(p/s)^4$. This emphasizes the importance of operating with the radius ratio p/s as near to 1 as physically possible.

Other Fourier Current Components

Because the current distribution of a real laboratory coil cannot realistically be represented as a single sine wave, it is of interest to compute the contribution to power absorption from Fourier components of the coil current other than the principal component. For an illustrative calculation it is assumed that

$$j^* = j\left(0.151\ e^{i4k_{01}z} + 0.422\ e^{i2k_{01}z} + 0.270\ e^{ik_{01}z}\right) \qquad |z| \leq a \tag{11a}$$

$$j^* = 0 \qquad z > a \tag{11b}$$

where $a = 2\pi/2k_{01}$, $k_{01} = 0.070$ per centimeter, $n_e = 5\times10^{11}$ per cubic centimeter,

$s/p = 3$ and $\omega = 2\pi \times 6.5 \times 10^6$ per second. This current distribution represents the three major Fourier components of the current profile shown in the inset of figure 11(a). This profile is the same as that in the ion-cyclotron resonance apparatus presently being used at the NASA Lewis Research Center. The principal wave number for this distribution is $2k_{01} = 0.140$ per centimeter, where $2k_{01}$ is approximately equal to the value of k_n which gives a maximum in the R/k_n^2 against k_n curve (fig. 5(b)). It is now interesting to examine the contributions to relative power absorption caused by the presence of the other Fourier components in the current distribution. It can be seen in figure 5(a) (R against k_n) that when $k_n = 4k_{01}$ R is larger than when $k_n = 2k_{01}$ (the principal wave number). Power transfer, however, is also proportional to the magnitude of the current squared; therefore, the contribution to power transfer from the $k_{01} = 4k_{01}$ Fourier component must be multiplied by $(0.151/0.422)^2 = 0.128$. This reduces the effect of the short wavelength component. The contribution from the long wavelength component ($k_{01} = k_{01}$) is also small because R for $k_n = k_{01}$ is smaller than R for $k_n = 2k_{01}$. The current weighting factor $(0.270/0.422)^2 = 0.630$ further reduces the contribution from the long wavelength component. Figure 11(a) shows relative power absorption when the effects of all three major Fourier components are included. It is seen that this curve is not drastically different from the curve in figure 4 where there was only one Fourier component.

Another current distribution which may be examined is the rectangular wave distribution shown in the inset of figure 11(b):

$$j^* = j\left(e^{ik_{01}z} + 0.54\, e^{i3k_{01}z} + \ldots\right) \qquad z \leq a \tag{12a}$$

$$j^* = 0 \qquad z > a \tag{12b}$$

The principal Fourier wave number components for this distribution are $k_{01} = 0.140$ per centimeter and $3k_{01} = 0.420$ per centimeter. Here again, R for $k_n = k_{01}$ is less than R for $k_n = 3k_{01}$, but the current weighting factor $(0.54/1)^2 = 0.292$ reduces the contribution from the short wavelength component. Contributions from other wavelength components are completely negligible for this rectangular wave distribution. Figure 12(b) shows relative power absorption for this distribution.

CONCLUDING REMARKS

Computer calculations based on the Stix equations (ref. 1) for power transfer to ion-cyclotron waves in a cold collisionless uniform plasma immersed in an axial magnetic field and excited by a radiofrequency coil show that radiofrequency power transfer by the plasma waves is relatively independent of density (for $n_e < 5 \times 10^{12}$ cm^{-3}) and increases approximately as the fourth power of the plasma radius. It has also been found that for any set of the parameters p, s, and n_e an optimum radiofrequency coil wavelength exists for maximum power transfer. The effect of displacement current for hydrogen plasmas with $B_0 < 100{,}000$ gauss has been shown to be very small. Also, the lowest order mode of oscillation of the plasma was found to contribute about 90 percent of the power transferred to the ion-cyclotron waves and to determine the basic shape of all the curves. Finally, it should be pointed out that the applicability of the

results presented in this report to a particular laboratory plasma depends on how well the laboratory plasma is represented by the model upon which the calculations were based.

Lewis Research Center,
National Aeronautics and Space Administration,
Cleveland, Ohio, December 14, 1965.

APPENDIX - COMPARISON OF FOURIER INTEGRAL THEORY WITH WITH FOURIER-BESSEL THEORY

Reference 2 gives the details of a technique employed by Stix prior to that of reference 1 for calculating power absorbed by the plasma model discussed in this report. To establish the difference between the two methods, calculations have been made for the following plasma using both techniques:

$$n_e = 5\times10^{11}\ \text{cm}^{-3}$$

$$s = 7.5\ \text{cm}$$

$$p = 7.5\ \text{cm}$$

$$\omega = 2\pi\times6.5\times10^{6}\ \text{sec}^{-1}$$

$$k_{01} = 0.140\ \text{cm}^{-1}$$

Results are compared in figure 12. For the reference 2 technique,

$$P^* = \left| \frac{-8\pi\omega}{c^2} \frac{1}{p} \left[\frac{1}{1 + \nu_n^{-2} p^{-2} (G^2 - 1)} \right] \left(\frac{k_{01} - k_n}{\nu_{01}^2 - \nu_n^2} \right) \right| S_r(\eta) \tag{13a}$$

$$G = k_{01} p \frac{K_0(k_{01}p)}{K_1(k_{01}p)} \tag{13b}$$

Stix's equations (ref. 2) contain absolute value signs on P^*, but the derivation of equation (13a) has been followed through carefully, and there appears to be no mathematical reason for inclusion of the absolute value signs. If the absolute signs are omitted in equation (13a), there is a value of Ω_{crit} (see fig. 12) above which the power absorbed by the plasma from the coil is negative (Ω_{crit} is determined by setting the denominator of equation (9) equal to zero with $k = k_{01}$). Thus, there is a breakdown in the usefulness of the technique of reference 2 at this point. Below Ω_{crit} the results of the two calculations are in agreement at only one value of Ω. This is the value of Ω for which $k_n = k_{01}$. In reference 2, the electric field under the finite length coil (for $0 < r < p$) was represented as a Fourier-Bessel series of nonorthogonal (but nearly orthogonal) functions. If the functions are assumed orthogonal in this range, the coefficients of the series can be calculated in closed form. This is the technique used by Stix in deriving equation (13a). It was thought that this assumption of orthogonality might lead to peculiarities in the calculations for relative power absorbed. However, Woollett (ref. 3) has correctly calculated the coefficients for the Bessel series and has found them to agree with the Stix coefficients to within a few percent. Thus, the nonorthogonality does not explain the difference between the reference 1 and reference 2 techniques. However, the conditions for the two models are slightly different. In reference 2 it was necessary to assume that the electric field was zero at the left end of the coil when a right running wave was assumed for the current sheet. This assumption eliminates a priori the

possibility of a left running wave in the plasma. In reference 1 no assumption was necessary on the electric field at the ends of the coil. In this case, the calculations show that a left running wave exists in the plasma. This wave is explained as a reflected wave caused by a mismatch between the natural modes of the plasma and the exciting current sheet. When $k_{01} = k_n$, the magnitude of the left running wave from reference 1 is zero. This is exactly the point at which the calculation on the two models agree. At $k_{01} = k_n$, the electric field is zero at the left end of the coil in reference 1 as well as in reference 2.

The technique of reference 1 has two other distinct advantages: First, it is not necessary to assume $s = p$ as in reference 2, and second, the technique of reference 1 can be easily applied to a plasma with a radial variation in density by using numerical integration. The reference 2 technique is considerably more difficult to apply to a variable density plasma.

REFERENCES

1. Stix, Thomas H.: The Theory of Plasma Waves. McGraw-Hill Book Co., Inc., 1962, pp. 82-101.

2. Stix, T. H.: Generation and Thermalization of Plasma Waves. Theoretical and Experimental Aspects of Controlled Nuclear Fusion. Vol. 31 of Proceeding of the Second United Nations International Conference on the Peaceful Uses of Atomic Energy, United Nations (Geneva), 1958, pp. 125-133.

3. Woollett, Richard R.: Error in Induced Electric Field Modes Under Stix Coil Resulting from Assumption of Orthogonality of Natural Plasma Modes. NASA TN D-3255, 1966.

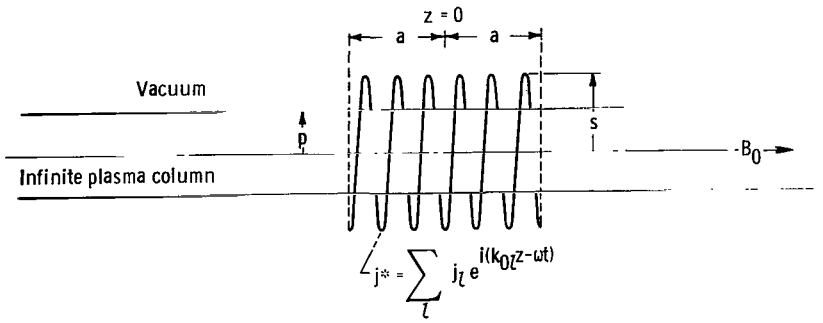

Figure 1. - Plasma column and radiofrequency coil configuration.

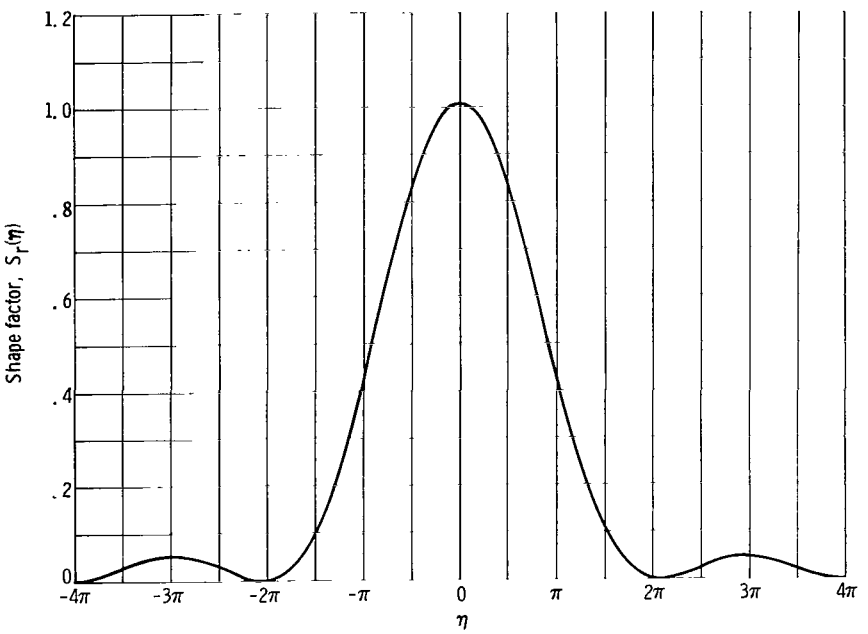

Figure 2. - Shape factor $S_r(\eta)$ as function of $\eta(\eta = 2(k_{0l} - k_n)a)$.

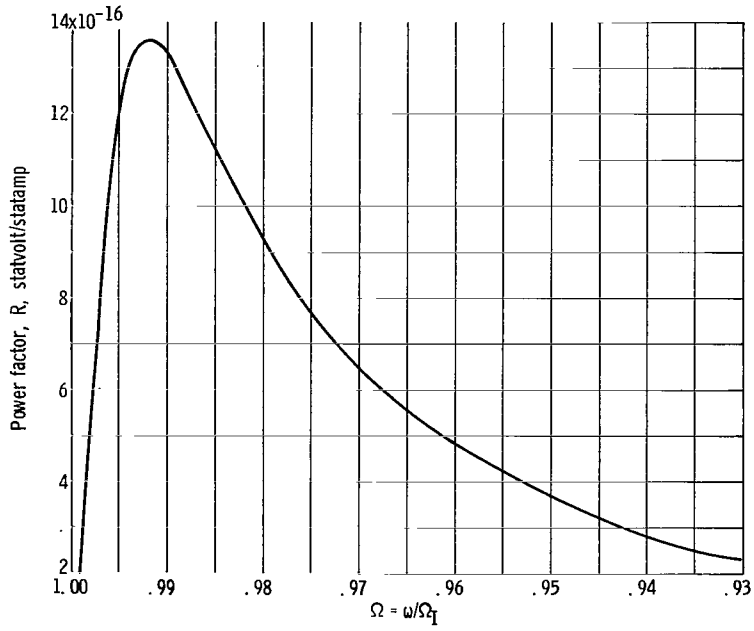

Figure 3. - Power factor R against Ω. Electron density, n_e, 5×10^{11} per cubic centimeter; plasma radius, 2.5 centimeters; radiofrequency coil radius, 7.5 centimeters.

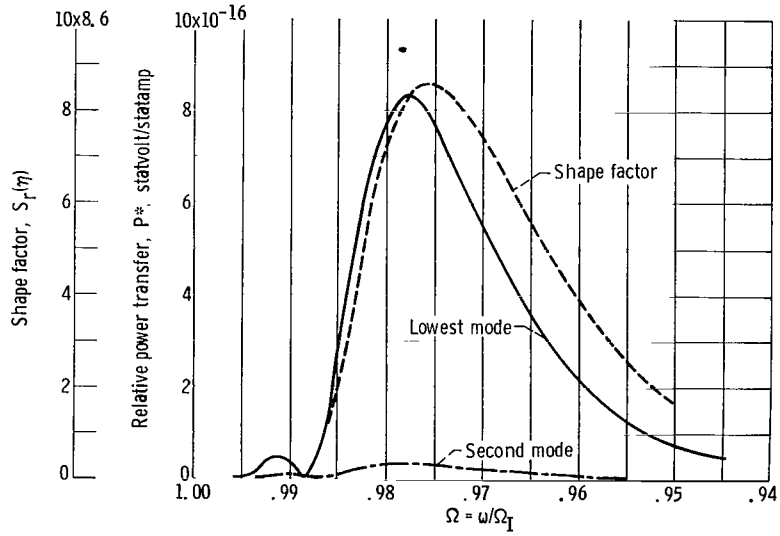

Figure 4. - Relative power P* and shape factor $S_r(\eta)$ as functions of Ω. Plasma radius, 2.5 centimeters; radiofrequency coil radius, 7.5 centimeters; electron density, 5×10^{11} per cubic centimeter; axial radiofrequency coil current propagation constant, 0.140 per centimeter.

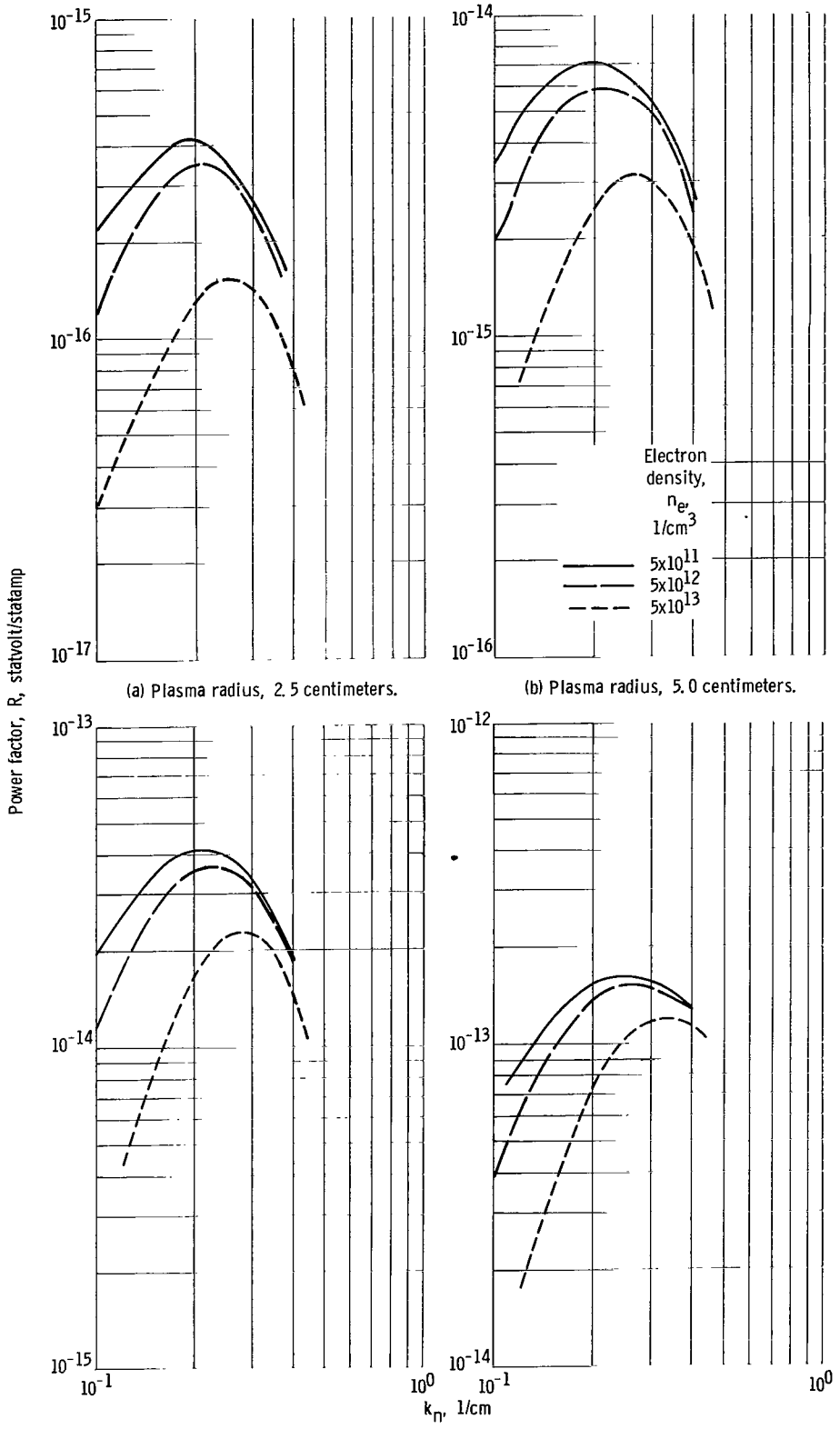

(a) Plasma radius, 2.5 centimeters.

(b) Plasma radius, 5.0 centimeters.

(c) Plasma radius, 7.5 centimeters.

(d) Plasma radius, 10.0 centimeters.

Figure 5. - Power factor R as function of k_n. Radiofrequency coil radius, 10 centimeters.

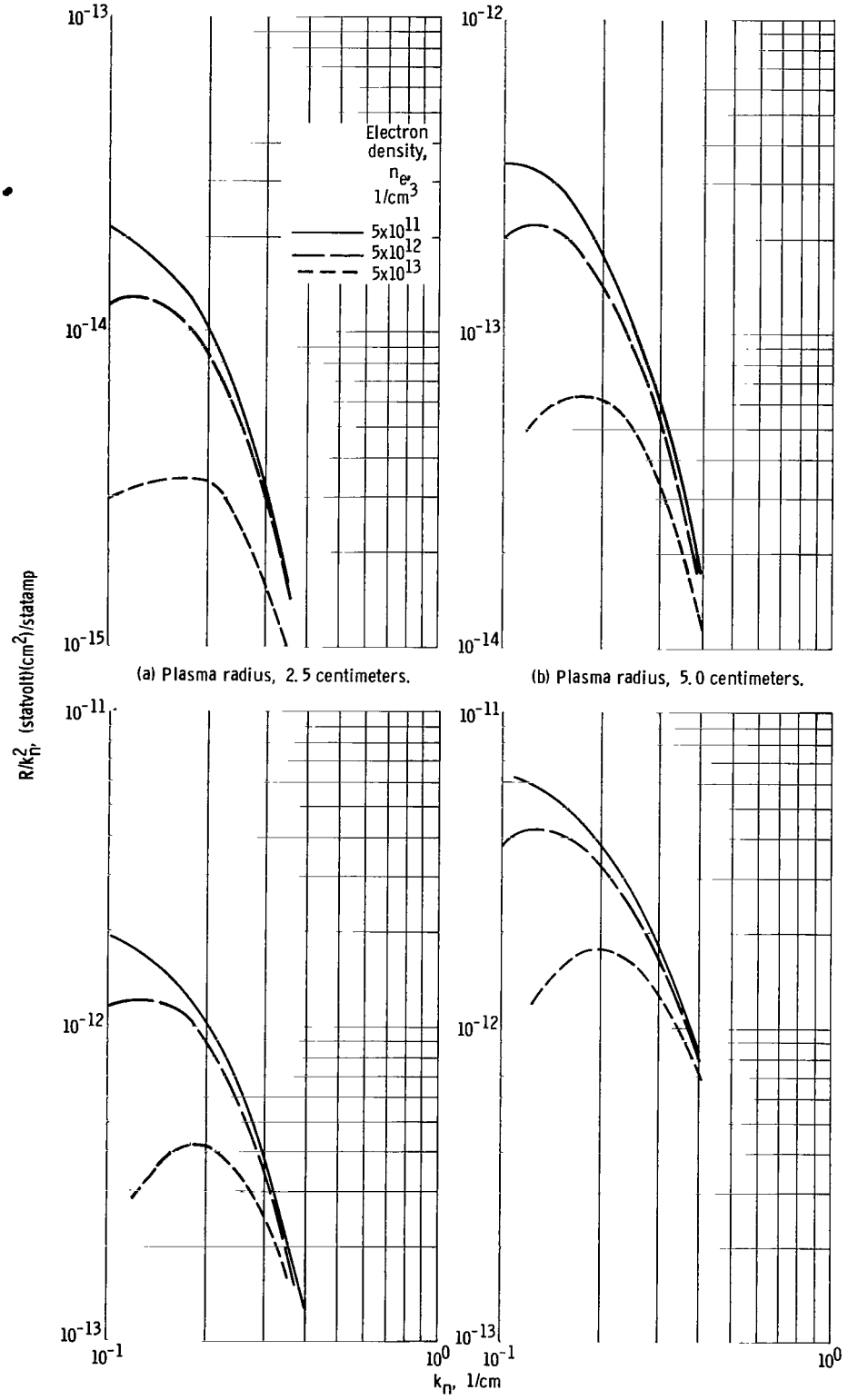

(a) Plasma radius, 2.5 centimeters.

(b) Plasma radius, 5.0 centimeters.

(c) Plasma radius, 7.5 centimeters.

(d) Plasma radius, 10.0 centimeters.

Figure 6. - Ratio R/k_n^2 as function of k_n. Radiofrequency coil radius, 10 centimeters.

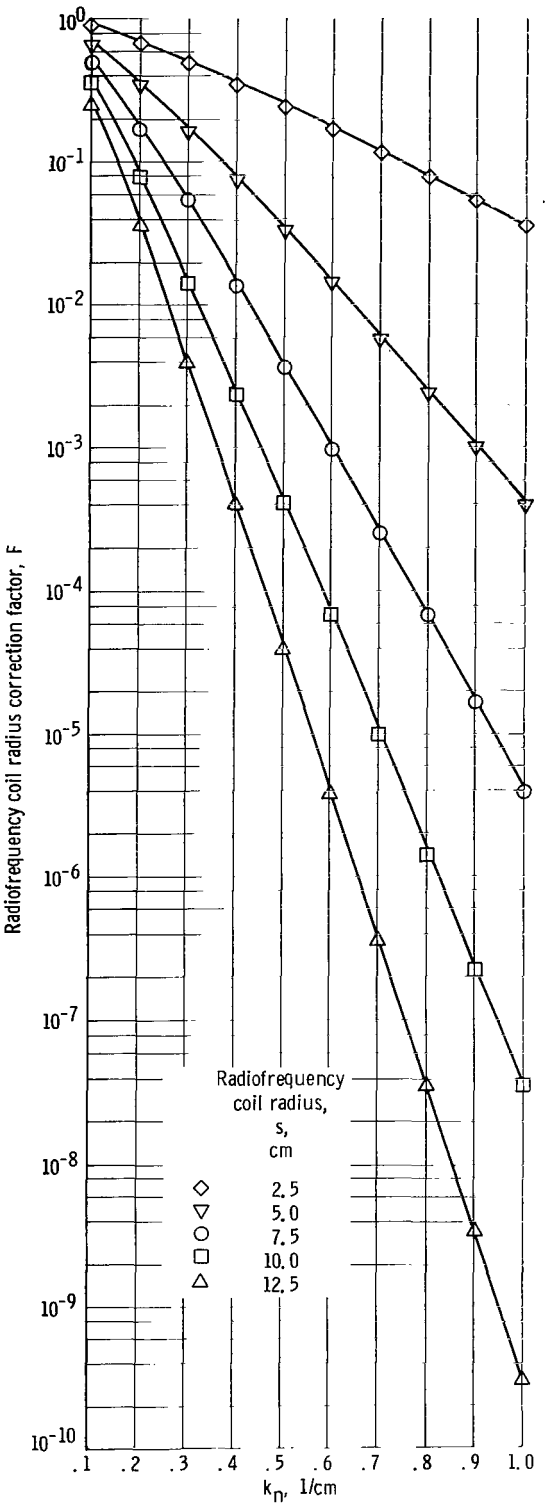

Figure 7. - Radiofrequency coil radius correction factor F as function of k_n.

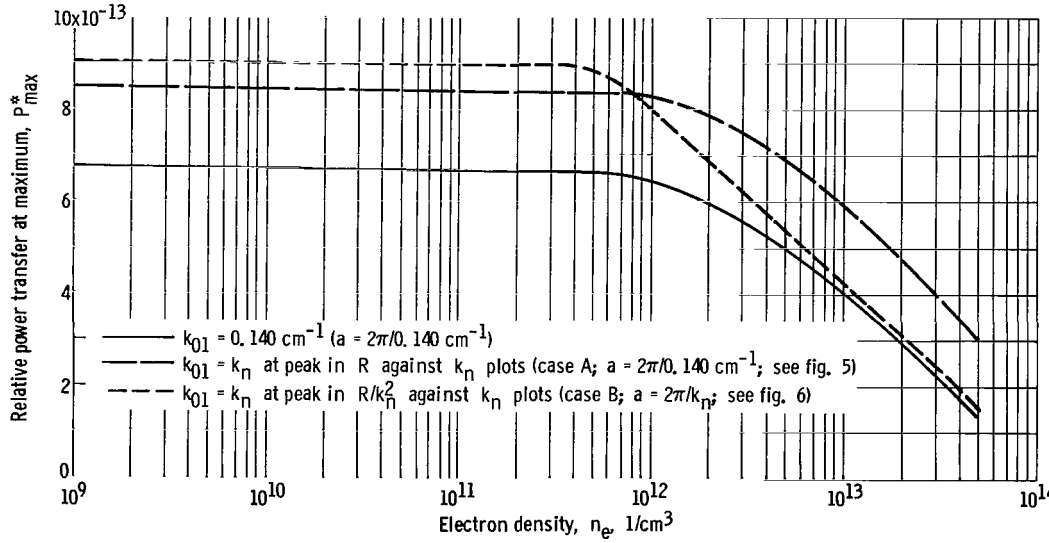

Figure 8. - Relative power transfer at maximum P^*_{max} as function of electron density n_e. Plasma radius, 2.5 centimeters, radiofrequency coil radius, 7.5 centimeters.

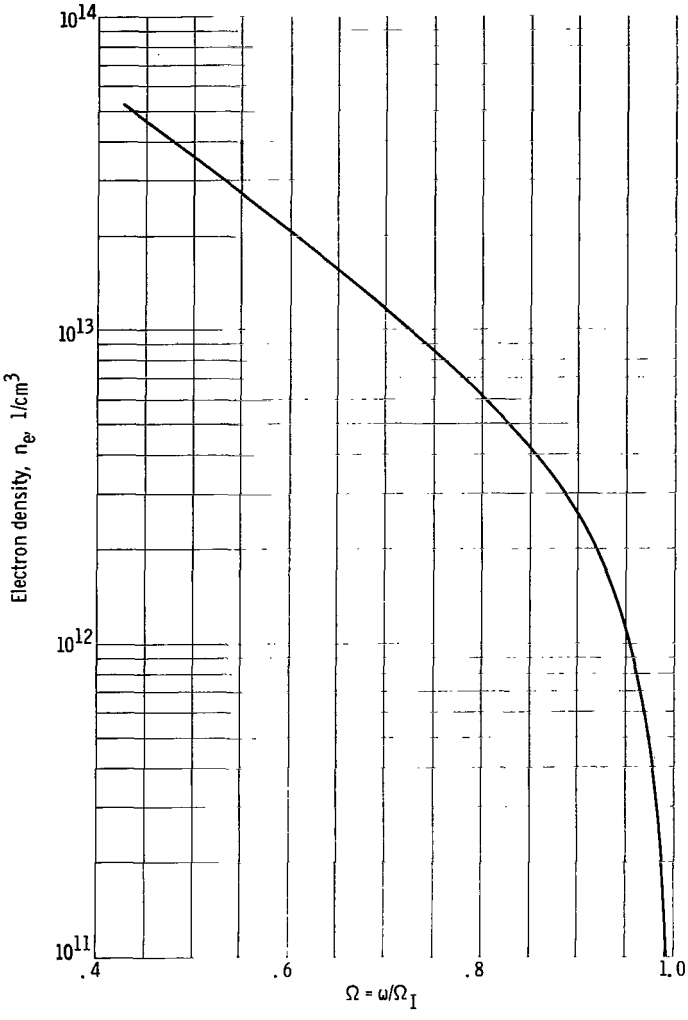

Figure 9. - The ratio Ω for maximum power as function of electron density n_e. Plasma radius, 2.5 centimeters; radiofrequency coil radius, 7.5 centimeters; axial radiofrequency coil current propagation constant, 0.140 per centimeter.

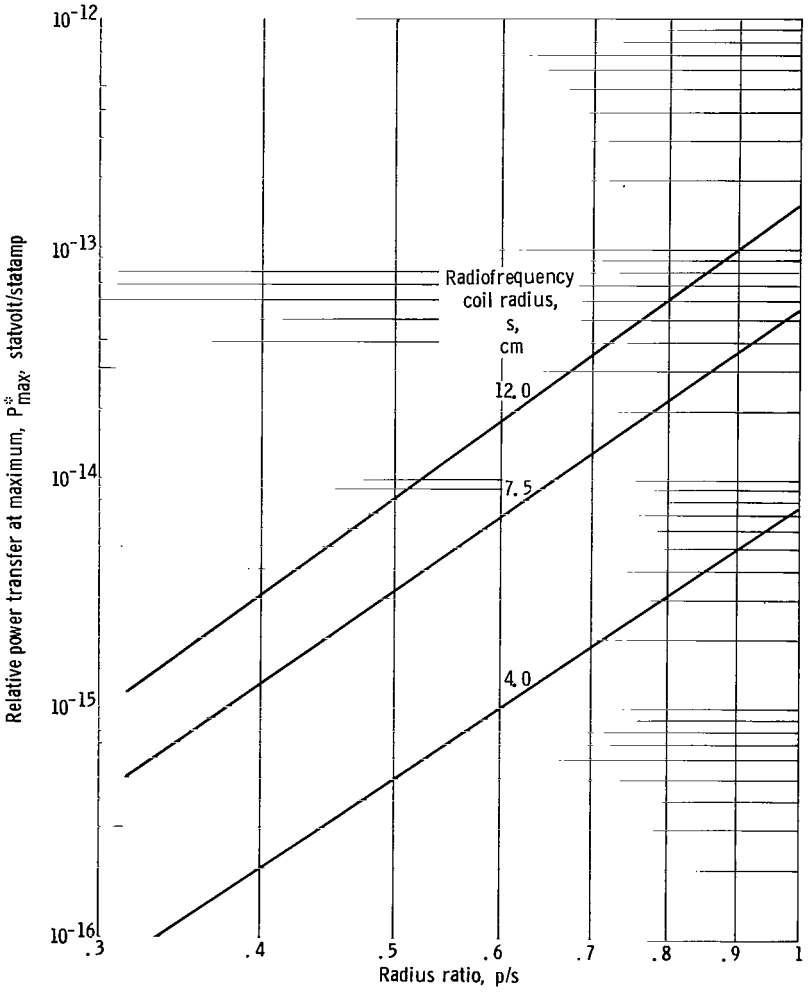

Figure 10. - Relative power P^* at maximum as function of radius ratio p/s. Electron density, 5×10^{11} per cubic centimeter; axial radiofrequency coil current propagation constant, 0.140 per centimeter.

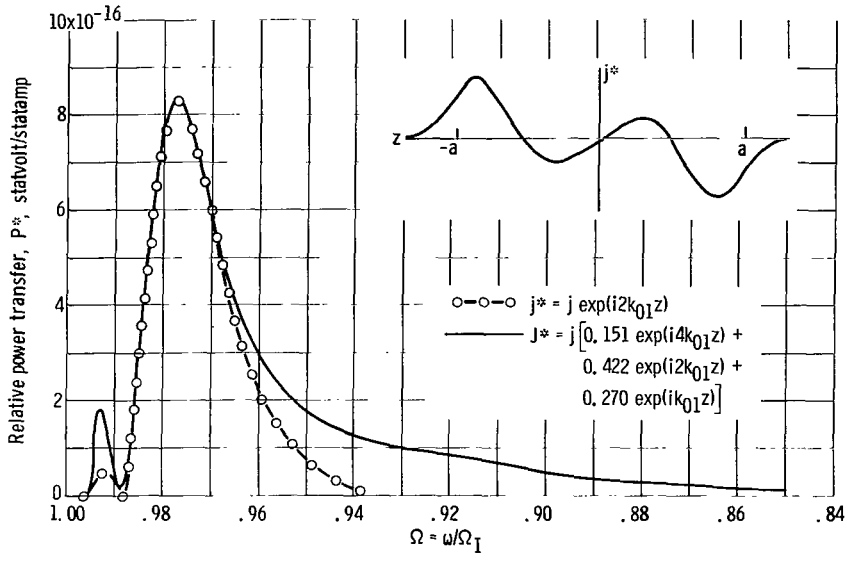

(a) Axial radiofrequency coil current propagation constant, 0.070 per centimeter.

Figure 11. - Relative power P* (lowest mode) as function of Ω. Plasma radius, 2.5 centimeters; radiofrequency coil radius, 7.5 centimeters; electron density, 5x10^{11} per cubic centimeter.

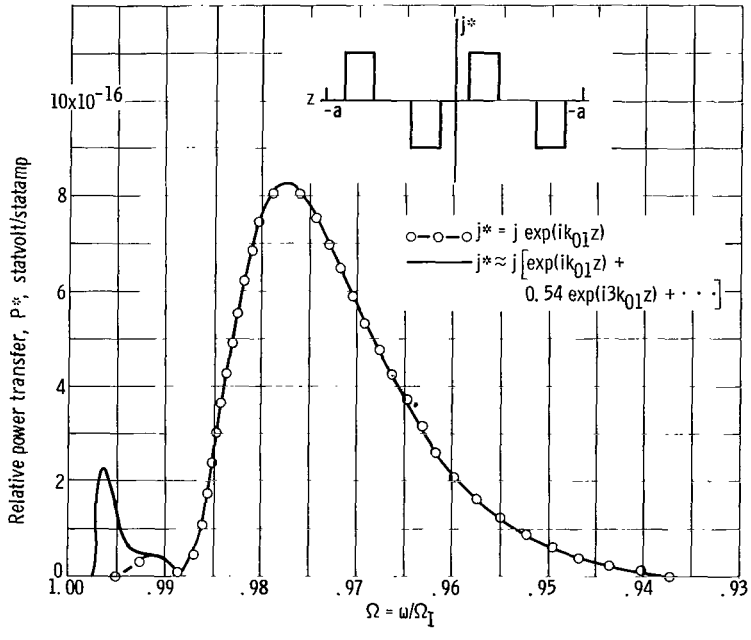

(b) Axial radiofrequency coil current propagation constant, 0.140 per centimeter.

Figure 11. - Concluded.

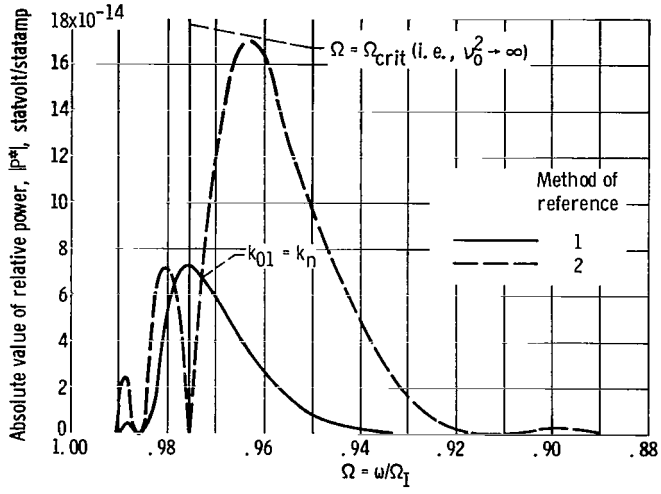

Figure 12. - Absolute value of relative power |P*| as function of Ω from both references 1 and 2. Plasma radius, 7.5 centimeters; radiofrequency coil current propagation constant, 0.140 per centimeter. (Method of ref. 2 gives negative P* for $\Omega > \Omega_{crit}$.)

"The aeronautical and space activities of the United States shall be conducted so as to contribute . . . to the expansion of human knowledge of phenomena in the atmosphere and space. The Administration shall provide for the widest practicable and appropriate dissemination of information concerning its activities and the results thereof."

—NATIONAL AERONAUTICS AND SPACE ACT OF 1958

NASA SCIENTIFIC AND TECHNICAL PUBLICATIONS

TECHNICAL REPORTS: Scientific and technical information considered important, complete, and a lasting contribution to existing knowledge.

TECHNICAL NOTES: Information less broad in scope but nevertheless of importance as a contribution to existing knowledge.

TECHNICAL MEMORANDUMS: Information receiving limited distribution because of preliminary data, security classification, or other reasons.

CONTRACTOR REPORTS: Technical information generated in connection with a NASA contract or grant and released under NASA auspices.

TECHNICAL TRANSLATIONS: Information published in a foreign language considered to merit NASA distribution in English.

TECHNICAL REPRINTS: Information derived from NASA activities and initially published in the form of journal articles.

SPECIAL PUBLICATIONS: Information derived from or of value to NASA activities but not necessarily reporting the results of individual NASA-programmed scientific efforts. Publications include conference proceedings, monographs, data compilations, handbooks, sourcebooks, and special bibliographies.

Details on the availability of these publications may be obtained from:

SCIENTIFIC AND TECHNICAL INFORMATION DIVISION

NATIONAL AERONAUTICS AND SPACE ADMINISTRATION

Washington, D.C. 20546